

Free Lunch for Gait Recognition: A Novel Relation Descriptor

Jilong Wang^{1,2,4}, Saihui Hou^{3,4}, Yan Huang², Chunshui Cao⁴, Xu Liu⁴, Yongzhen Huang^{3,4}, Liang Wang^{2*}

¹University of Science and Technology of China

²Institute of Automation, Chinese Academy of Sciences

³Beijing Normal University

⁴WATRIX.AI

jilongw@mail.ustc.edu.cn, {yhuang, liangwang}@nlpr.ia.ac.cn

{housaihui, huangyongzhen}@bnu.edu.cn, {chunshui.cao, xu.liu}@watrix.ai

Abstract

Gait recognition is to seek correct matches for query individuals by their unique walking patterns. However, current methods focus solely on extracting individual-specific features, overlooking inter-personal relationships. In this paper, we propose a novel **Relation Descriptor** that captures not only individual features but also relations between test gaits and pre-selected anchored gaits. Specifically, we reinterpret classifier weights as anchored gaits and compute similarity scores between test features and these anchors, which re-expresses individual gait features into a similarity relation distribution. In essence, the relation descriptor offers a holistic perspective that leverages the collective knowledge stored within the classifier’s weights, emphasizing meaningful patterns and enhancing robustness. Despite its potential, relation descriptor poses dimensionality challenges since its dimension depends on the training set’s identity count. To address this, we propose the Farthest Anchored-gait Selection to identify the most discriminative anchored gaits and an Orthogonal Regularization to increase diversity within anchored gaits. Compared to individual-specific features extracted from the backbone, our relation descriptor can boost the performances nearly without any extra costs. We evaluate the effectiveness of our method on the popular GREW, Gait3D, CASIA-B, and OUMVLP, showing that our method consistently outperforms the baselines and achieves state-of-the-art performances.

1. Introduction

Gait recognition aims at identifying people at a long distance by their unique walking patterns [28]. As an identification task in vision, the essential goal of it is to learn

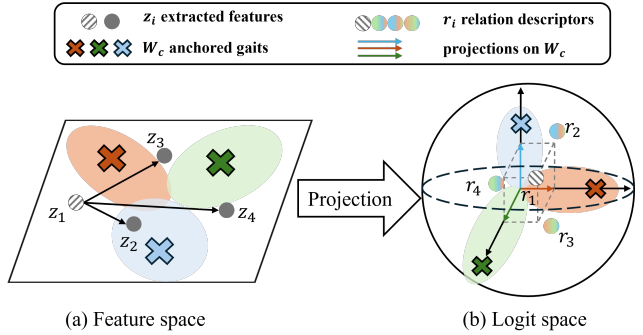


Figure 1. The comparison of identity-specific embedding and relation-specific logit. (a) Conventional gait recognition utilizes the extracted feature for the final identification. (b) Incorporating with well-trained anchored gaits’ vectors, gait representations could be converted into relation descriptors that describe the similarity to anchored semantic directions.

the distinctive and invariant representations from the physical and behavioral human walking characteristics. With the boom of deep learning, gait recognition has achieved great progress [6, 10, 11, 29, 37], yielding impressive results on public datasets.

Reappraising an established pipeline of gait recognition [10, 16, 21, 34], prior work typically involves a *feature extractor* for obtaining unique gait features of individual walking sequences and usually utilizes a *classifier* [22] for accurate identity classification. In common practice, since test identities are unseen at the training stage, the classifier for training set classification loses its significance for test identities and is usually discarded at the inference stage. However, the classifier occupies the majority of the network’s weights especially when the number of training classes is large, for example, 92.1% and 75.1% of total weights in GaitBase [10] on GREW [44] and OUMVLP [30], respectively. Thus, a natural question would arise:

*Corresponding Author

whether the well-trained weights in classifiers for the training set are really useless for inference?

In this work, we draw wisdom from human beings: **human nature is the ensemble of social relations** instead of abstraction inherent in every single individual [18]. This philosophical point of view provides a new perspective on recognition. Intuitively, providing relation descriptions within a whole group, such as ‘tallest person among them’, makes it easier to identify a person compared to just giving an inherent feature like “7 feet tall”. This kind of description presents the composite relationships of a person rather than just individual traits. Inspired by it, we assume that gait goes beyond just an aggregation of individual features; it can also be expressed through the relationships with the gait features of others. These relationships may involve aspects of similarity, dissimilarity, common traits, *etc.*, reflecting patterns and variations of gait within a population. As shown in Fig. 1, with several preselected person’s gaits as anchored references, other gaits can be described as a distribution of differences/similarities with these anchored reference gaits.

To get a relation description, a set of anchored gaits should be first determined. Therefore, *we rethink the role of the classifier by reinterpreting its weights as the well-defined gait prototype for each person in the training set, essentially serving as anchored gaits (AGs)*. Hence, a person’s gait can be re-expressed by the relations between its extracted feature and the well-defined anchored gaits. To be specific, the normalized dot product of gait features and anchored gaits represents similarities [14] distribution, constructing a new **Relation Descriptor (RD)**. Each dimension of RD indicates the similarity of gait features to a specific AG. Since the weights in the classifier denote the well-defined gait feature in the training set, RD can be seen as a projection of gait features in these semantic directions. In essence, *the RD offers a holistic perspective that leverages the collective knowledge stored within the classifier’s weights*. Thereby, RD brings two natural benefits: 1) emphasizing meaningful features instead of noise and 2) more robust and generalizable ability.

However, directly employing RD poses two challenges, *i.e.*, **dimension expansion** and **dimension shrinking**, as the number of AGs in the classifier is dependent on the count of training identities. When numerous AGs are selected, such as 20000 and 5153 in GREW [44] and OU-MVLP [30], the dimension of the RD can surpass that of the original embedding. This expansion results in increased storage costs and practical challenges in real-world applications. This is because the more AGs there are, the more dimensions are needed to represent the relationships accurately. On the other hand, too few AGs may lead to a reduced variety of gait patterns and variations within the RD. This shrinking of dimensionality could diminish the

descriptor’s ability to capture the diverse nuances of different individuals’ gaits.

Therefore, balancing the quantity of AGs to avoid excessive expansion or shrinking while retaining meaningful information is a key consideration in the design and application of the RD. In our work, we propose two techniques to address these challenges.

For the problem of **dimension expansion**, we find that not all identities in the training set are needed since there would be many similar identity prototypes, which results in many redundant relationships. Thus, we assume that the most discriminative combination of AGs in the latent space should be the one with the largest spanning space, *i.e.*, the maximum divergence. We introduce a Farthest Anchored-gait Selection (FAS) algorithm to select the most discriminative set of AGs. Then, a Singular Value Decomposition (SVD) would be adopted to further reduce the dimensions of the selected AGs without losing information.

For the problem of **dimension shrinking**, we find that few identities in the training set would lead to an overfitting problem which makes AGs less discriminative. Therefore, we propose an Orthogonal Regulation Loss (ORL) for better classifier training, which encourages the classifier’s weights to be orthogonal to each other, increasing the diversity among AGs. As a result, the RD can better reflect the distinct characteristics of different individuals’ gaits even with a small set of AGs.

We rigorously evaluate our proposed approach on established benchmark datasets including GREW [44], Gait3D [43], CASIA-B [38], and OU-MVLP [30], consistently demonstrating its superiority over conventional baseline methods.

To summarize, the contributions of our work can be outlined in three aspects:

- (i) We propose a novel descriptor for gait recognition, capturing not only individual features but also relationships among well-trained anchored gaits, which enhances recognition performance without extra costs.
- (ii) We address the challenges of dimension expansion and shrinking by the Farthest Anchored-gaits Selection algorithm and Orthogonal Regulation Loss, improving efficiency and discrimination.
- (iii) We evaluate the effectiveness of our proposed method on four popular datasets, and the extensive experimental results demonstrate the superior performance of our approach.

2. Related Work

2.1. Gait Recognition

Gait recognition aims to identify people by their unique representation of their gait characteristics. According to their type of inputs, current works can be roughly grouped

into model-based and appearance-based categories. Model-based methods [1, 4, 19, 41] pay attention to modeling the static structures and dynamic relations among key points of the human body. Appearance-based [6, 11, 15, 16, 21, 29] approaches methods directly obtain spatial-temporal features from binary gait silhouettes. Thanks to the contributions of prior work, a typical pipeline of gait recognition has been established. It primarily consists of four components: 1) a spatial-temporal feature extractor to get individual inherent features (CNN [6, 7, 10, 11, 21, 34], Transformer [9, 35], GCN [12, 31], *etc.*), 2) a temporal pooling module to aggregate sequence’s feature (MaxPooling [6], MeanPooling [29], GeM [21], *etc.*), 3) a multi-scale module to obtain fine-grained information (HPP [6], attention [7, 8], body parsing, *etc.*), 4) and metric learning loss functions to enhance features’ discrimination (Triplet Loss [27], Cross-entropy Loss [40], *etc.*).

However, previous works have emphasized extracting individual-specific gait features, thereby overlooking the relationships among different gait sequences. In this work, we propose a novel perspective that a person’s gait characteristics can also be described by the relationships between their own gait and other anchor gaits. Furthermore, we unearth collective knowledge hidden behind the classifier.

2.2. Open-set Recognition

Open-set recognition (OSR) is a classification task with the additional requirement of rejecting inputs from unknown classes in the latent space [25]. The data labeled as ‘unknown’ classes should be far from the ‘known’ training classes in the latent space. In the area of OSR, researchers mainly use the logits from the classifier to measure the distance between ‘unknown’ data and ‘known’ clusters. OpenMax [3] models all known classes by their logits as a single cluster and re-calibrates softmax scores according to the distance between input and other cluster centers. Several following works [13, 23, 24, 26] propose many mechanisms to improve the distance-based measures, such as data augmentation or introducing an ‘other’ class. Recent works [5, 32] find that a good close-set classifier can directly boost the performance of open-set recognition, which prompts a reconsideration of the role of classifiers.

Existing works in OSR also highlight the importance of classifiers, yet, they primarily differ from our work in two aspects: (1) The classifier in OSR is needed for ‘known’ class classification, while we drop the concept of classification and consider training identities as our AGs; (2) OSR emphasizes the logits of unseen classes should be far from that of ‘known’ classes, while we advocate the discriminative capacity of logits. Overall, our work proposes a brand new perspective for the usage of classifiers.

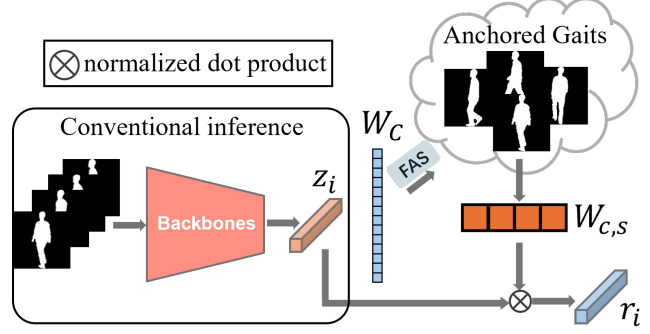


Figure 2. The overview of our pipeline. The anchored gaits are selected from the well-trained classifier and the final representation is mapped into a cosine similarity space.

3. Our Approach

In this work, we revisit the role of classifiers in the testing phase of gait recognition and thus propose a new gait descriptor. We find the well-trained weights in the classifier can be regarded as anchored gaits, and the relationship between the gait feature and the set of anchored gaits can be used as a discriminative descriptor. In this section, we first introduce our new pipeline of relation-based gait recognition and then explain the proposed relation descriptor and the way of its construction. Next, we thoroughly analyze two crucial challenges brought by RD, *i.e.*, dimension expansion and shrinking, and introduce several proposed mechanisms to address them.

3.1. Pipeline

We follow a typical gait recognition procedure [10, 21] during the training phase. Given a dataset with data-label pairs $\mathcal{D} = \{(x_i, y_i)\}$ where x_i denotes a gait sequence and $y_i \in C$ indicates the class label of x_i . \mathcal{D} will be divided into training set D_{train} and test set D_{test} , where $C_{train} \cap C_{test} = \emptyset$. The Ω is a feature extractor that embeds the gait sequences into a d -dimensional latent space, where $z_i = \Omega(x_i)$ is the extracted representation. The goal of training Ω on D_{train} is to learn a discriminative transformation from x_i to $z_i \in \mathbb{R}^d$, satisfying that the intra-class variations are smaller than inter-class differences.

A common practice [7, 8, 10, 16, 21] uses a combination of triplet loss [27] and cross-entropy loss [40] to get a more discriminative Ω . A BNNeck [22] with a weights matrix $W_c \in \mathbb{R}^{d \times C}$ would be introduced during the training stage for the classification task. In our work, we adopt a cosine similarity classifier [14] in BNNeck. The $r_i \in \mathbb{R}^C$ indicates the normalized dot product results of z_i with all identities’ gait prototypes, where the larger r_i^j is, the more similar z_i and W_c^j are.

Unlike prior works, we advocate to use r_i for the final individual identification, thereby we keep the classi-

fier in the test phase, as in Fig. 2. To address the mentioned challenges brought RD, we further adopt our Farthest Anchored-gait Selection algorithm and Orthogonal Regulation Loss for dimension expansion and dimension shrinking, respectively. Finally, with the help of the well-trained classifier and our proposed methods, relation descriptors r_i that achieve **higher performance** can be obtained nearly **without extra costs**, and their dimensions are **the same or less** than that of z_i .

3.2. A Novel Relationship Descriptor

We now introduce the core idea of our paper: gait goes beyond just an aggregation of individual features; it can also be expressed through the relationships with the gait features of others.

To be specific, gait is usually seen as a unique walking pattern for each individual, influenced by various factors including body structure, posture, stride length, and more. Previous works run identification on this level, assuming each dimension of z_i refers to unique individual features and the Euclidean distances between these features indicate the similarity between different identities' gaits. It can be formulated as

$$\text{dist}(z_a, z_b) = \sqrt{\sum_i^d (z_a^i - z_b^i)^2} \quad (1)$$

However, gait can be also expressed by comparing the relationships between the gait features of different individuals, which involves aspects of similarity, dissimilarity, and common traits. For example, the person I 's gait can be described as 0.2 of *anchored gait* 1, 0.7 of AG2, 0.1 of AG3, -0.5 of AG4, and so on. Here we use cosine similarity for relationship measurement. As a result, a novel descriptor of person I can be $r_1 = [0.2, 0.7, 0.1, -0.5, \dots]$, which denotes the relationship between other anchored persons. We call this descriptor as **Relationship Descriptor**. Based on it, Euclidean distances can be also defined as

$$\text{dist}(r_a, r_b) = \sqrt{\sum_i^{|AG|} (r_a^i - r_b^i)^2} \quad (2)$$

where $|AG|$ is the number of AGs.

Noting that the discriminative ability of the RD heavily relies on the set of AGs. The higher the diversity of patterns and variations within the AGs group is, the stronger the discrimination capability of the RD is. To get a set of well-defined AGs, we set our sights on the classifier. Since the cross-entropy loss [40] would minimize the negative log-probability of an input's ground truth class, the weights in the classifier would encapsulate specific gait representations only tied to each identity in the training set. However, the cross-entropy loss only constrains the relative magnitudes of logits, so the absolute values of logits lack clear significance. Hence, we employ the *cosine similarity classifier* that constrains output range is $[-1, 1]$ which also provides

explicit semantic meaning for the absolute values. As a result, the output of the Euclidean distance is also constrained within the range $[0, 2\sqrt{|AG|}]$. For the sake of conciseness, all classifiers mentioned in the following text refer to the cosine similarity classifier. According to the above discussion, the well-trained weights in the classifier can be regarded as our AGs. Their normalized dot product with test gait features represents similarity, signifying the relationship descriptors of test identities. It can be formulated as

$$r_i = \frac{W_c^T \cdot z_i}{\|W_c\| * \|z_i\|} \quad (3)$$

where the $\|W_c\|$ is the 2-norm of W_c along the d dimension. And the Eq. 2 can be rewritten as

$$d(r_a, r_b) = \sqrt{\sum_j^C \frac{W_{c,j}^T}{\|W_{c,j}\|} \cdot \left(\frac{z_a}{\|z_a\|} - \frac{z_b}{\|z_b\|} \right)} \quad (4)$$

The proposed RD can be obtained without any extra costs, and the knowledge hidden behind the classifier be further unearthed.

Compared to EigenFace and FisherFace. EigenFace [39] and FisherFace [2] show that face images can be linearly represented by a collection of base features obtained by PCA or LDA, in other words, all face images can be described by the 'proportions' of all the base features. They are also implementations of our core idea of taking relations as descriptors. However, they are easily affected by the co-variants and are mainly employed on a small training set due to the heavy computational costs. Unlike these methods, the AGs are more discriminative bases in the latent space, which is learned by a non-linear model on a higher semantic level.

3.3. Challenge: Dimension Expansion

As we discussed above, the AGs can be seen as a set of semantic bases in the latent space, but, the number of bases relies on the number of training identities. When training on a large-scale dataset, the dimension of W_c is inevitably expanding, incurring augmented storage costs and redundant information. Therefore, the combination of AGs should be carefully selected.

What is a good combination of anchored gaits? The latent space is a manifold determined by the training data, and the class weights can be seen as bases that span the manifold. Thus, in order to maintain the discriminative ability, the manifold spanned by the combination of selected AGs needs to be as consistent as possible with the original manifold. Additionally, when the $C > d$, there are many linearly related bases in the classifier which can be removed.

Based on the above discussion, we assume that the most discriminative combination of AGs should be the one

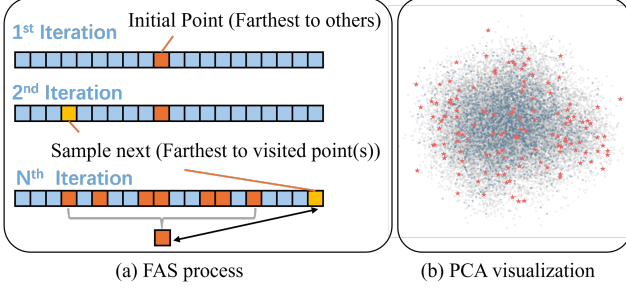


Figure 3. (a) Visualization of FAS process. (b) PCA visualization of training data (gray), W_c (dark blue) in classifier, and $W_{c,s}$ (red) selected by FAS.

with the largest spanning space, *i.e.*, the maximum within-divergence.

How to select good anchored gaits. Selecting a subset of AGs with maximum within-divergence from all weights in the classifier is an NP-hard problem, which is generally difficult to solve in polynomial time. Hence, we propose a heuristic method, called Farthest Anchored-gait Selection (FAS), to solve this problem.

Given weights in the classifier $\{W_{c,1}, W_{c,2}, \dots, W_{c,C}\}$, we use iterative FAS to choose a combination of N weights $\{W_{c,s1}, W_{c,s2}, \dots, W_{c,sN}\}$ as AGs, where the $W_{c,sj}$ is the farthest weights from the barycenter of the set $\{W_{c,s1}, W_{c,s2}, \dots, W_{c,sj-1}\}$. The final selected weights are denoted by $W_{c,s} \in \mathbb{R}^{d \times N}$. The distances are computed by Euclidean distances. FAS is a greedy algorithm described in Algorithm 1 and a visualization of this process is shown in Figure 3.

The internal mechanism of FAS is based on the assumption that the farthest weight from the selected weights contains the most different semantic information, thus, it is good for increasing the diversity of the combination anchored gaits. Compared to the original W_c , the $W_{c,s}$ collects the discriminative anchored gaits and removes redundant ones.

How to reduce the final dimension. Even though the FAS would filter out some useless weight, the number of anchored gaits is usually larger than the original embeddings' dimension. Luckily, we know the dimension of $W_{c,s}$ can be reduced to d without information loss when $d < |AG|$ by Singular Value Decomposition (SVD).

SVD is performed on the selected weight matrix $W_{c,s}$ to decompose the feature:

$$W_{c,s} = U \Sigma V^T \quad (5)$$

where $\Sigma \in \mathbb{R}^{d \times N}$ rectangular diagonal singular value matrix, $U \in \mathbb{R}^{d \times d}$ and $V \in \mathbb{R}^{N \times N}$ are left and right orthogonal singular vector matrices, respectively. Then we select only top- k weights from the $W_{c,s}$ by

$$W_{c,r} = U[:, :k] \Sigma[:, k:k] \quad (6)$$

Algorithm 1 Pseudo-code of FAS in a PyTorch-like style.

```
# cdist(): matrix-wise L2 distance
dist = cdist(W_c, W_c.t())
# the farthest weight from all others
farthest = dist.sum(-1).argmax()
W_cs[0] = W[farthest]
# remove the selected basis from W
W_c.remove(farthest)

for i in range(1, N):
    dist = cdist(W_cs.mean(dim=1), W.t())
    farthest = dist.sum(-1).argmax()
    W_cs[i] = W[farthest]
    W_c.remove(farthest)
```

where $W_{c,r} \in \mathbb{R}^{d \times k}$ is the dimension-reduced AGs.

3.4. Challenge: Dimension Shrinking

When there are only a few identities in the training stage, especially $C < d$, the classifier is easily over-fitted, thus, the class weights would be less discriminative. On the other hand, too few AGs lead to a reduced variety of gait patterns and variations within the RD. This shrinking of dimensionality could diminish the RD's ability to capture the diverse nuances of different individuals' gaits.

To tackle this limitation, we propose an orthogonal regulation loss (ORL) to minimize the correlation between different identity's weights, increasing the diversity among AGs, which can be formulated as

$$L_{ORL} = \|W_c^T W_c - I\|_1 \quad (7)$$

where $I \in \mathbb{R}^{C \times C}$.

By enhancing the separability between anchor gaits, the RD can better reflect the distinct characteristics of different individuals' gaits even with a reduced number of anchors. A more carefully designed method is sure to further improve the performance, but it is not the priority of this paper. Note that ORL is only used in small datasets with few identities.

4. Experiments

4.1. Datasets

GREW [44]. GREW is the largest outdoor dataset, containing 26,345 subjects with 128,671 sequences captured from 882 cameras. According to its official partition, GREW is divided into three subsets, *i.e.*, the training set with 20,000 subjects, the validation set with 345 subjects, and the test set with 6,000 subjects.

Gait3D [43]. Gait3D is an in-the-wild dataset, containing 4000 subjects with over 25,000 sequences captured from 39 cameras. To facilitate a fair comparison with other algorithms, Gait3D provides an official protocol that 3000 subjects are used for training while the remaining 1000 subjects are for test.

Table 1. Rank-1 accuracy (%), Rank-5 accuracy (%), Rank-10 accuracy (%), and Rank-20 accuracy (%) on the GREW dataset.

Methods	Rank-1	Rank-5	Rank-10	Rank-20
PoseGait [20]	0.2	1.0	2.2	4.3
GaitGraph [31]	1.3	3.5	5.1	7.5
GEINet [29]	6.8	13.4	17.0	21.0
TS-CNN [36]	13.6	24.6	30.2	37.0
GaitSet [6]	46.3	63.6	70.3	76.8
GaitPart [11]	44.0	60.7	67.3	73.5
GaitGL [21]	47.3	63.6	69.3	74.2
MGN [33]	44.5	61.3	67.7	72.7
CSTL [17]	50.6	65.9	71.9	76.9
MTSGait [42]	55.3	71.3	76.9	81.6
GaitBase [10]	60.1	75.7	80.5	84.4
GaitBase+ours	65.5	78.7	83.3	86.3

OU-MVLP [30]. The OU-MVLP is the largest indoor gait dataset under a fully controlled environment. It includes 10,307 subjects under normal walking conditions and 14 views uniformly distributed between $[0^\circ, 90^\circ]$ and $[180^\circ, 270^\circ]$. Each view embodies 2 sequences. In our work, we adopt the wildly-used protocol that 5153 subjects are used for training and the rest are taken for the test.

CASIA-B [38]. It is one of the most popular gait datasets, which contains 124 subjects from 11 view angles uniformly ranging from $(0^\circ, 180^\circ)$. For each subject under each view, there are 10 sequences under 3 walking conditions, namely normal walking (NM), carrying bags (BG), and wearing a coat or jacket (CL). For fairness, our work follows the popular partition constructed by [6]. To be specific, the first 74 subjects are used for training and the remaining 50 subjects are reserved for the test.

4.2. Implementation Details

We utilize GaitBase [10] as our main baseline on Gait3D, GREW, and OU-MVLP. And GaitGL [21] with a cosine similarity classifier is used on CASIA-B. Most experiments are directly using the pre-trained weights of these models. Moreover, we also reproduce some methods in our ablation study. For these reproduced models [6, 11], we add an extra BNNeck cosine similarity classifier for them, and the temperature in cross-entropy loss is set to 16. For other training details of these methods, we strictly follow their official settings, and our code is based on OpenGait [10].

Hyperparameters. The number of N in FAS is set to 74, 1024, 2048, and 8192 in the CASIA-B, Gait3D, OU-MVLP, and GREW, respectively. The k in SVD is set to the same as embedding dimension d . ORL is only used to train the model on CASIA-B and its coefficient is set to 1.

Table 2. Rank-1 accuracy(%), mAP, and mINP comparison on Gait3D. The bold number denotes the best performances.

Method	Venue	Gait3D		
		Rank-1	mAP	mINP
PoseGait	PR20	0.2	0.5	0.3
GaitGraph	ICIP21	6.3	5.2	2.4
GaitSet	AAAI19	36.7	30.0	17.3
GaitPart	CVPR20	28.2	21.6	12.4
GLN [16]	ECCV20	31.4	24.7	13.6
GaitGL	ICCV21	29.7	22.3	13.3
CSTL	ICCV21	11.7	5.6	2.6
SMPLGait [43]	CVPR22	46.3	37.2	22.2
GaitBase	CVPR23	64.6	55.2	30.4
GaitBase+ours	-	70.1	61.9	36.2

4.3. Performance Comparison

GREW. We compare the performance of the proposed method with several gait recognition methods on the GREW dataset and show experimental results in Tab. 1. GREW is collected under an unconstrained condition, thus it contains lots of unpredictable external covariants, such as occlusion and bad segmentation. As a result, gait sequences in the test set may be encoded by some unseen covariant that further produces meaningless gait representation. From Tab. 1, we can see the gait recognition methods that perform well on indoor datasets meet a large performance degradation. It shows the gait representations encoded by only individual features are not robust enough. By replacing our relation descriptor incorporating FAS and SVD, our method elevate the accuracy of the state-of-the-art GaitBase by 5.4%, 3.0%, 2.8%, and 1.9% on Rank-1, Rank-5, rank-10, and rank-20, respectively. It is worth noting that our method adds no extra parameters and the dimension of the final gait representation is the same as the original GaitBase. The experimental results indicate that the relation descriptor is more discriminative and robust in real-world scenarios.

Gait3D. Gait3D is also an unconstrained dataset. The comparison of prevailing competing methods is illustrated in Tab. 2, demonstrating that our proposed method exhibits superior performance compared to previous methods by a considerable margin. Since our method utilizes the relationship between test gait and well-defined anchored gaits, it will be less affected by unseen external covariants. As a result, our method outperforms all prevailing methods and can boost the performance of GaitBase by 5.4%, 6.7%, and 5.8% on Rank-1, mAP, and mINP, respectively.

OU-MVLP and CASIA-B. Since both OU-MVLP and CASIA-B are collected in a fully-constrained laboratory environment, their training and testing sets possess nearly identical covariates. The effects of covariates can be well

Table 3. Averaged rank-1 accuracy (%) on OU-MVLP, excluding identical-view cases.

Methods	Prove View															Mean
	0°	15°	30°	45°	60°	75°	90°	180°	195°	210°	225°	240°	225°	270°		
GEINet	23.2	38.1	48.0	51.8	47.5	48.1	43.8	27.3	37.9	46.8	49.9	45.9	45.7	41.0	42.5	
GaitSet	79.3	87.9	80.0	90.1	88.0	88.7	87.7	81.8	86.5	89.0	89.2	87.2	87.6	86.2	87.1	
GaitPrart	82.6	88.9	90.8	91.0	89.7	89.9	89.5	85.2	88.1	90.0	90.1	89.0	89.1	88.2	88.7	
GLN	83.8	90.0	91.0	91.2	90.3	90.0	89.4	85.3	89.1	90.5	90.6	89.6	89.3	88.5	89.2	
GaitGL	84.9	90.2	91.1	91.5	91.1	90.8	90.3	88.5	88.6	90.3	90.4	89.6	89.5	88.8	89.7	
GaitBase	85.6	90.7	91.5	91.8	90.9	90.7	90.2	87.5	90.1	90.8	91.1	90.2	90.0	89.5	90.0	
GaitBase+ours	87.3	91.4	91.9	92.1	91.4	91.2	90.8	89.0	90.7	91.2	91.3	90.7	90.6	90.1	90.7	

Table 4. Ablation study on relation descriptors (RD), Farthest Anchored-gait Selection (FAS), and Orthogonal Regulation Loss (ORL) on CASIA-B and Gait3D.

	RD	FAS	ORL	CASIA-B	Gait3D
				Mean Acc. ↑	Rank-1 Acc. ↑
#1				91.8	64.6
#2	✓			90.6 ^{↓-1.2}	68.8 ^{↑+2.2}
#3	✓	✓		N/A	70.1 ^{↑+5.5}
#4	✓		✓	92.5 ^{↑+0.7}	N/A

Table 5. Model agnostic results on Gait3D dataset.

Rank-1	Methods			
Acc.	GaitSet	GaitPart	GaitGL	GaitBase
Baseline	36.7	28.2	29.7	64.6
w. Ours	42.5 ^{↑+5.8}	38.0 ^{↑+9.8}	37.1 ^{↑+7.4}	70.1 ^{↑+5.5}

eliminated during the training stage. Hence, directly using individual gait features as representation can achieve promising accuracy. However, we find our method can still boost the baseline performance on these two datasets, especially when the number of training identities is large. On the OU-MVLP, our method boosts GaitBase accuracy across all viewpoints by using relation descriptors computed on 2500 anchored gaits. On the CASIA-B, our methods improve the average accuracy of GaitGL by 0.7%. Notably, the dimension of the relation descriptors on CASIA-B is 74 since only 74 identities are in the training set. Thus, our method achieves higher accuracy with fewer feature dimensions. The experiments have demonstrated that relationship descriptors exhibit discriminative capability comparable to or higher than individual gait features. Furthermore, as the number of candidate anchor gaits increases, the performance of the relationship descriptors improves.

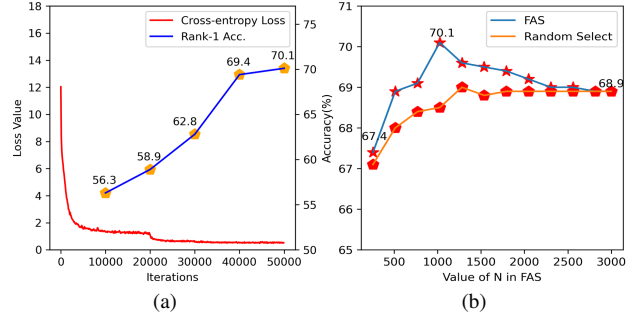


Figure 4. (a) The cross-entropy loss and accuracy curves of GaitBase on Gait3D. (b) Ablation study on the number of selected anchored gaits in FAS on Gait3D.

4.4. Ablation Study

In this subsection, we provide the ablation study of each component in our method on the CASIA-B and Gait3D.

Analysis of RD, FAS, and ORL. The ablation result is illustrated in Tab. 4. Note that the FAS is only employed for datasets where the number of identities C in the training set exceeds the output dimension d . In contrast, ORL is only applied on datasets where $C < d$. Here is the analysis: 1) from experiment #2, RD improves the baseline by 2.2% on Gait3D but degrades the performance on CASIA-B by 1.2% due to fewer anchored gaits; 2) Comparing #4 with #2, adding ORL to generate more separate anchored gaits brings improvement on CASIA-B, which shows the importance of anchored gaits; 3) Comparing #4 with #2, the selected combination of anchored gaits can further improve the recognition accuracy, which proves that our FAS would produce a better combination. Overall, the ablation result verifies the effectiveness of our proposed methods.

Analysis of model agnostic results. As shown in Tab. 5, we conduct experiments on Gait3D with four popular methods, including GaitSet, GaitPart, GaitGL, and GaitBase. Since GaitSet and GaitPart don't use cross-entropy loss, we train an extra cosine similarity classifier for them. Then for these four methods, we adopt FAS to select 1024 anchored gaits

Table 6. Averaged rank-1 accuracy (%) on CASIA-B, excluding identical-view cases.

Gallery NM#1-4		Prove View											
Probe		0°	18°	36°	54°	72°	90°	108°	126°	144°	162°	180°	Mean
NM#5-6	GaitSet	90.8	97.9	99.4	96.9	93.6	91.7	95.0	97.8	98.9	96.8	85.8	95.0
	GaitPart	94.1	98.6	99.3	98.5	94.0	92.3	95.9	98.4	99.2	97.8	90.4	96.2
	MT3D	95.7	98.2	99.0	97.5	95.1	93.9	96.1	98.6	99.2	98.2	92.0	96.7
	GaitBase	-	-	-	-	-	-	-	-	-	-	-	97.6
	GaitGL	96.0	98.3	99.0	97.9	96.9	95.4	97.0	98.9	99.3	98.8	94.0	97.4
	GaitGL+ours	95.5	98.6	98.9	97.9	96.5	94.8	97.5	98.8	98.8	98.3	94.2	97.3
BG#1-2	GaitSet	83.8	91.2	91.8	88.8	83.3	81.0	84.1	90.0	82.2	84.4	79.0	87.2
	GaitPart	89.1	94.8	96.7	95.1	88.3	84.9	89.0	93.5	96.1	93.8	85.8	91.5
	MT3D	91.0	95.4	97.5	94.2	92.3	86.9	91.2	95.6	97.3	96.4	86.6	93
	GaitBase	-	-	-	-	-	-	-	-	-	-	-	94.0
	GaitGL	92.6	96.6	96.8	95.5	93.5	89.3	92.2	96.5	98.2	96.9	91.5	94.5
	GaitGL+ours	94.0	96.3	96.6	95.8	93.4	88.8	92.8	97.1	98.6	96.8	89.2	94.5
CL#1-2	GaitSet	61.4	75.4	80.7	77.3	72.1	70.1	71.5	73.5	73.5	68.4	50.0	70.4
	GaitPart	70.7	85.5	86.9	83.3	77.1	72.5	76.9	82.2	83.8	80.2	66.5	78.7
	GaitBase	-	-	-	-	-	-	-	-	-	-	-	77.4
	MT3D	76.0	87.6	89.8	85.0	81.2	75.7	81.0	84.5	85.4	82.2	68.1	81.5
	GaitGL	76.6	90.0	90.3	87.1	84.5	79.0	84.1	87.0	87.3	84.4	69.5	83.6
	GaitGL+ours	77.6	90.6	92.2	89.0	85.0	79.9	87.0	89.1	89.6	82.3	70.9	84.9

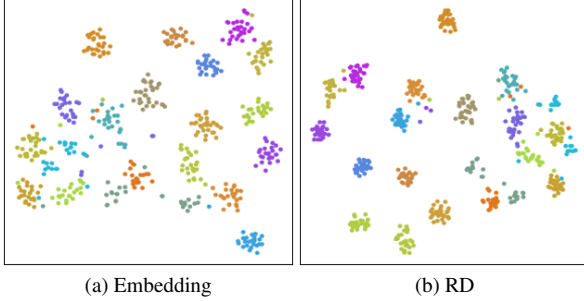


Figure 5. T-SNE visualization on Gait3D test set with randomly selected 20 classes. One color denotes a class.

from their classifiers and then adopt SVD to keep the dimension of the relation descriptor the same as their original embeddings. The results show that the proposed method can improve performance regardless of the baseline backbones or network structures. The model agnostic property further verifies the superior discriminative capacity of the relation descriptor.

Analysis of the value N in FAS. As we mentioned above, not all weights in the classifier contribute to better recognition performance. From Fig. 4b, we can conclude that: first, the performance of relation descriptor relies on the pre-selected anchored gaits; second, it is important to note that selecting too few or all of the weights doesn't necessarily lead to performance improvement, where the curve first rises and then falls as N is increased. Compared to random

selection, FAS can bring consistent performance improvement, which proves our assumption that the most discriminative combination of anchored gaits should be the one with the largest spanning space.

Analysis of the relationship between classifier convergence and accuracy. The relation descriptor depends on the well-defined weights in the classifier, which is based on the assumption that each weight represents a typical gait representation. The cross-entropy loss requires separating the weights of different identities. Hence, the weights in a classifier with better convergence can better represent distinct gait features, leading to superior results. This phenomenon can be observed in Fig. 4a.

4.5. Visualization

. We visualize the feature distribution of models' original embeddings and RD on Gait3D test set with 20 randomly selected classes. By comparing Figs. 5a and 5b, it shows that the intra-class variation is further reduced and the inter-class distance is hence enlarged by our relation descriptor. The visualization demonstrates that RD is a more discriminative representation. Furthermore, we visualize the anchored gaits selection results of FAS on the GaitBase in the Gait3D training set. As shown in Fig. 3, We can observe that the weights are mostly concentrated in the center, while the selected weights are mainly distributed on the periphery. It proves the effectiveness of our FAS.

5. Conclusion

In this paper, we propose a novel Relationship Descriptor for gait recognition. The RD captures not only individual features but also the relationships between the test sample and predefined anchor gaits. In essence, the RD offers a holistic perspective that leverages the collective knowledge stored within the classifier’s weights. Despite its potential, we also notice dimensionality challenges caused by RD. FAS and ORL are carefully designed to solve these issues and further boost recognition performance. Overall, we hope these new insights could spur further research in the gait community.

References

- [1] Gunawan Ariyanto and Mark S. Nixon. Model-based 3d gait biometrics. In *2011 International Joint Conference on Biometrics (IJCB)*, pages 1–7, 2011. 3
- [2] Peter N. Belhumeur, Joao P Hespanha, and David J. Kriegman. Eigenfaces vs. fisherfaces: Recognition using class specific linear projection. *IEEE Transactions on pattern analysis and machine intelligence*, 19(7):711–720, 1997. 4
- [3] Abhijit Bendale and Terrance E Boult. Towards open set deep networks. In *Proceedings of the IEEE conference on computer vision and pattern recognition*, pages 1563–1572, 2016. 3
- [4] R. Bodor, A. Drenner, D. Fehr, O. Masoud, and N. Papanikolopoulos. View-independent human motion classification using image-based reconstruction. *Image Vision Comput.*, 27(8):1194–1206, jul 2009. 3
- [5] Jun Cen, Di Luan, Shiwei Zhang, Yixuan Pei, Yingya Zhang, Deli Zhao, Shaojie Shen, and Qifeng Chen. The devil is in the wrongly-classified samples: Towards unified open-set recognition. *arXiv preprint arXiv:2302.04002*, 2023. 3
- [6] Hanqing Chao, Kun Wang, Yiwei He, Junping Zhang, and Jianfeng Feng. GaitSet: Cross-view gait recognition through utilizing gait as a deep set. *IEEE transactions on pattern analysis and machine intelligence*, 44(7):3467–3478, 2021. 1, 3, 6
- [7] Huanzhang Dou, Pengyi Zhang, Wei Su, Yunlong Yu, and Xi Li. Metagait: Learning to learn an omni sample adaptive representation for gait recognition. In *European Conference on Computer Vision*, pages 357–374. Springer, 2022. 3
- [8] Huanzhang Dou, Pengyi Zhang, Wei Su, Yunlong Yu, Yining Lin, and Xi Li. Gaitgci: Generative counterfactual intervention for gait recognition. In *Proceedings of the IEEE/CVF Conference on Computer Vision and Pattern Recognition*, pages 5578–5588, 2023. 3
- [9] Chao Fan, Saihui Hou, Yongzhen Huang, and Shiqi Yu. Exploring deep models for practical gait recognition. *arXiv preprint arXiv:2303.03301*, 2023. 3
- [10] Chao Fan, Junhao Liang, Chuanfu Shen, Saihui Hou, Yongzhen Huang, and Shiqi Yu. Opengait: Revisiting gait recognition towards better practicality. In *Proceedings of the IEEE/CVF Conference on Computer Vision and Pattern Recognition (CVPR)*, pages 9707–9716, June 2023. 1, 3, 6
- [11] Chao Fan, Yunjie Peng, Chunshui Cao, Xu Liu, Saihui Hou, Jiannan Chi, Yongzhen Huang, Qing Li, and Zhiqiang He. GaitPart: Temporal part-based model for gait recognition. In *2020 IEEE/CVF Conference on Computer Vision and Pattern Recognition (CVPR)*, pages 14213–14221, 2020. 1, 3, 6
- [12] Yang Fu, Shibe Meng, Saihui Hou, Xuecai Hu, and Yongzhen Huang. Gpgait: Generalized pose-based gait recognition. *arXiv preprint arXiv:2303.05234*, 2023. 3
- [13] ZongYuan Ge, Sergey Demyanov, Zetao Chen, and Rahil Garnavi. Generative openmax for multi-class open set classification. *arXiv preprint arXiv:1707.07418*, 2017. 3
- [14] Spyros Gidaris and Nikos Komodakis. Dynamic few-shot visual learning without forgetting. In *Proceedings of the IEEE conference on computer vision and pattern recognition*, pages 4367–4375, 2018. 2, 3
- [15] J. Han and Bir Bhanu. Individual recognition using gait energy image. *IEEE Transactions on Pattern Analysis and Machine Intelligence*, 28(2):316–322, 2006. 3
- [16] Saihui Hou, Chunshui Cao, Xu Liu, and Yongzhen Huang. Gait lateral network: Learning discriminative and compact representations for gait recognition. In *Computer Vision - ECCV 2020: 16th European Conference, Glasgow, UK, August 23-28, 2020, Proceedings, Part IX*, pages 382–398, Berlin, Heidelberg, 2020. Springer-Verlag. 1, 3, 6
- [17] Xiaohu Huang, Duowang Zhu, Hao Wang, Xinggang Wang, Bo Yang, Botao He, Wenyu Liu, and Bin Feng. Context-sensitive temporal feature learning for gait recognition. In *Proceedings of the IEEE/CVF International Conference on Computer Vision*, pages 12909–12918, 2021. 6
- [18] Alison M Jaggar. *Feminist politics and human nature*. Rowman & Littlefield, 1983. 2
- [19] Worapan Kusakunniran, Qiang Wu, Hongdong Li, and Jian Zhang. Multiple views gait recognition using view transformation model based on optimized gait energy image. In *2009 IEEE 12th International Conference on Computer Vision Workshops, ICCV Workshops*, pages 1058–1064, 2009. 3
- [20] Rijun Liao, Shiqi Yu, Weizhi An, and Yongzhen Huang. A model-based gait recognition method with body pose and human prior knowledge. *Pattern Recognition*, 98:107069, 2020. 6
- [21] Beibei Lin, Shunli Zhang, and Xin Yu. Gait recognition via effective global-local feature representation and local temporal aggregation. In *Proceedings of the IEEE/CVF International Conference on Computer Vision (ICCV)*, pages 14648–14656, October 2021. 1, 3, 6
- [22] Hao Luo, Wei Jiang, Youzhi Gu, Fuxu Liu, Xingyu Liao, Shenqi Lai, and Jianyang Gu. A strong baseline and batch normalization neck for deep person re-identification. *IEEE Transactions on Multimedia*, 22(10):2597–2609, 2019. 1, 3
- [23] Dimity Miller, Niko Sunderhauf, Michael Milford, and Feras Dayoub. Class anchor clustering: A loss for distance-based open set recognition. In *Proceedings of the IEEE/CVF Winter Conference on Applications of Computer Vision*, pages 3570–3578, 2021. 3

- [24] Lawrence Neal, Matthew Olson, Xiaoli Fern, Weng-Keen Wong, and Fuxin Li. Open set learning with counterfactual images. In *Proceedings of the European Conference on Computer Vision (ECCV)*, pages 613–628, 2018. 3
- [25] Walter J Scheirer, Anderson de Rezende Rocha, Archana Sapkota, and Terrance E Boulton. Toward open set recognition. *IEEE transactions on pattern analysis and machine intelligence*, 35(7):1757–1772, 2012. 3
- [26] Patrick Schlachter, Yiwen Liao, and Bin Yang. Open-set recognition using intra-class splitting. In *2019 27th European signal processing conference (EUSIPCO)*, pages 1–5. IEEE, 2019. 3
- [27] Florian Schroff, Dmitry Kalenichenko, and James Philbin. Facenet: A unified embedding for face recognition and clustering. In *2015 IEEE Conference on Computer Vision and Pattern Recognition (CVPR)*, pages 815–823, 2015. 3
- [28] Chuanfu Shen, Shiqi Yu, Jilong Wang, George Q Huang, and Liang Wang. A comprehensive survey on deep gait recognition: algorithms, datasets and challenges. *arXiv preprint arXiv:2206.13732*, 2022. 1
- [29] Kohei Shiraga, Yasushi Makihara, Daigo Muramatsu, Tomio Echigo, and Yasushi Yagi. Geinet: View-invariant gait recognition using a convolutional neural network. In *2016 International Conference on Biometrics (ICB)*, pages 1–8, 2016. 1, 3, 6
- [30] Noriko Takemura, Yasushi Makihara, Daigo Muramatsu, Tomio Echigo, and Yasushi Yagi. Multi-view large population gait dataset and its performance evaluation for cross-view gait recognition. *IPSJ Transactions on Computer Vision and Applications*, 10(1), 2018. 1, 2, 6
- [31] Torben Teepe, Ali Khan, Johannes Gilg, Fabian Herzog, Stefan Hörmann, and Gerhard Rigoll. Gaitgraph: Graph convolutional network for skeleton-based gait recognition. In *2021 IEEE International Conference on Image Processing (ICIP)*, pages 2314–2318. IEEE, 2021. 3, 6
- [32] Sagar Vaze, Kai Han, Andrea Vedaldi, and Andrew Zisserman. Open-set recognition: A good closed-set classifier is all you need? *arXiv preprint arXiv:2110.06207*, 2021. 3
- [33] Guanshuo Wang, Yufeng Yuan, Xiong Chen, Jiwei Li, and Xi Zhou. Learning discriminative features with multiple granularities for person re-identification. In *Proceedings of the 26th ACM international conference on Multimedia*, pages 274–282, 2018. 6
- [34] Ming Wang, Xianda Guo, Beibei Lin, Tian Yang, Zheng Zhu, Lincheng Li, Shunli Zhang, and Xin Yu. Dygait: Exploiting dynamic representations for high-performance gait recognition. *arXiv preprint arXiv:2303.14953*, 2023. 1, 3
- [35] Qian Wu, Ruixuan Xiao, Kaixin Xu, Jingcheng Ni, Boxun Li, and Ziyao Xu. Gaitformer: Revisiting intrinsic periodicity for gait recognition. *arXiv preprint arXiv:2307.13259*, 2023. 3
- [36] Zifeng Wu, Yongzhen Huang, Liang Wang, Xiaogang Wang, and Tieniu Tan. A comprehensive study on cross-view gait based human identification with deep cnns. *IEEE transactions on pattern analysis and machine intelligence*, 39(2):209–226, 2016. 6
- [37] Shiqi Yu, Haifeng Chen, Edel B. García Reyes, and Norman Poh. Gaitgan: Invariant gait feature extraction using generative adversarial networks. In *2017 IEEE Conference on Computer Vision and Pattern Recognition Workshops (CVPRW)*, pages 532–539, 2017. 1
- [38] Shiqi Yu, Daoliang Tan, and Tieniu Tan. A framework for evaluating the effect of view angle, clothing and carrying condition on gait recognition. In *18th international conference on pattern recognition (ICPR'06)*, volume 4, pages 441–444. IEEE, 2006. 2, 6
- [39] Jun Zhang, Yong Yan, and Martin Lades. Face recognition: eigenface, elastic matching, and neural nets. *Proceedings of the IEEE*, 85(9):1423–1435, 1997. 4
- [40] Zhilu Zhang and Mert Sabuncu. Generalized cross entropy loss for training deep neural networks with noisy labels. *Advances in neural information processing systems*, 31, 2018. 3, 4
- [41] Guoying Zhao, Guoyi Liu, Hua Li, and Matti Pietikainen. 3d gait recognition using multiple cameras. In *7th International Conference on Automatic Face and Gesture Recognition (FGR06)*, pages 529–534. IEEE, 2006. 3
- [42] Jinkai Zheng, Xinchun Liu, Xiaoyan Gu, Yaoqi Sun, Chuang Gan, Jiyong Zhang, Wu Liu, and Chenggang Yan. Gait recognition in the wild with multi-hop temporal switch. In *Proceedings of the 30th ACM International Conference on Multimedia*, pages 6136–6145, 2022. 6
- [43] Jinkai Zheng, Xinchun Liu, Wu Liu, Lingxiao He, Chenggang Yan, and Tao Mei. Gait recognition in the wild with dense 3d representations and a benchmark. In *Proceedings of the IEEE/CVF Conference on Computer Vision and Pattern Recognition*, pages 20228–20237, 2022. 2, 5, 6
- [44] Zheng Zhu, Xianda Guo, Tian Yang, Junjie Huang, Jiankang Deng, Guan Huang, Dalong Du, Jiwen Lu, and Jie Zhou. Gait recognition in the wild: A benchmark. In *Proceedings of the IEEE/CVF international conference on computer vision*, pages 14789–14799, 2021. 1, 2, 5